LETTER • OPEN ACCESS

Universal excitonic superexchange in spin-orbit-coupled Mott insulators

To cite this article: Chao-Kai Li and Gang Chen 2022 *EPL* **139** 56001

A Letters Journal Exploring the Frontiers of Physics

September 2022

EPL, **139** (2022) 56001
doi: 10.1209/0295-5075/ac8612

www.epljournal.org

Universal excitonic superexchange in spin-orbit-coupled Mott insulators

Chao-Kai Li and Gang Chen[(a)]

Department of Physics and HKU-UCAS Joint Institute for Theoretical and Computational Physics at Hong Kong, The University of Hong Kong - Hong Kong, China and
The University of Hong Kong Shenzhen Institute of Research and Innovation - Shenzhen 518057, China

received 29 May 2022; accepted in final form 2 August 2022
published online 17 August 2022

Abstract – We point out the universal presence of the excitonic superexchange in spin-orbit-coupled Mott insulators. It is observed that the restriction to the lowest spin-orbit-entangled "J" states may sometimes be insufficient to characterize the microscopic physics, and the virtual excitonic processes via the upper "J" states provide an important correction to the superexchange. We illustrate this excitonic superexchange from a two-dimensional $5d$ iridate Sr_2IrO_4 and explain its physical consequences such as the orbital-like coupling to the external magnetic flux and the nonlinear magnetic susceptibility. The universal presence of the excitonic superexchange in other spin-orbit-coupled Mott insulators such as $3d$ Co-based Kitaev magnets and even f electron rare-earth magnets is further discussed.

Introduction. – There has been a great interest in the field of spin-orbit-coupled correlated materials [1], ranging from the correlated spin-orbit-coupled metals or semimetals to the spin-orbit-coupled Mott insulators. The latter cover the $4d/5d$ magnets like Kitaev materials, iridates, osmates [2–14], $4f$ rare-earth magnets [15–21], or even $3d$ Co-based Kitaev magnets and Ni-based diamond antiferromagnets that are of some recent interest [22–31]. In these materials, the local moments are formed by the spin-orbit-entangled "J" or "J_{eff}" states. In the study of the superexchange interactions between the local moments, the prevailing assumption was to consider the pairwise superexchange interaction between the neighboring local moments from the lowest J states, and the treatment was to carry out the perturbation theory of the extended Hubbard model. The result from this assumption and treatment were somewhat successful, especially in the systems where the lowest J states are very well separated from the excited or upper J states and at the same time the Mott gap is large.

In many of these spin-orbit-coupled Mott insulators, the spin-orbit coupling is not really a dominant energy scale especially in $3d$ or $4d$ transition metal compounds, and thus the energy separation between the lowest J states and the upper J states is not quite large compared to the hoppings and magnetic interactions, though it may involve both the crystal field effect and the spin-orbit coupling. In rare-earth magnets, this energy separation is defined by the crystal field and can sometimes be small compared to the exchange energy scale. Moreover, the famous Kitaev materials like iridates and α-$RuCl_3$ are not good insulator as the charge gaps in these materials are not quite large [12,32–34]. In this work, we explore the excitonic superexchange process that involves the upper J states virtually and provide an important and universal correction to the superexchange interaction in the spin-orbit-coupled Mott insulators. The excitonic process refers to the tunneling of the electron from the lowest J states to the upper J states between the neighboring sites.

What was our previous knowledge about the superexchange interaction of the spin-orbit-coupled Mott insulators? For the $J = 1/2$ moments, due to the absence of the continuous rotational symmetry, all possible symmetry-allowed pairwise exchange interactions, including Heisenberg, Dzyaloshinskii-Moriya and pseudo-dipole interactions [35], appear in the exchange matrix and are

[(a)]E-mail: gangchen@hku.hk (corresponding author)

likely to be equally important. Moreover, the diagonal entry of the exchange matrix from the Heisenberg and the pseudo-dipole interactions can yield the Kitaev [3] or Kitaev-like anisotropic compass interaction [2,3]. For the larger J moments (*e.g.*, $J = 3/2$ or 2), due to the larger physical Hilbert space and the strong accessibility via the spin-orbit entanglement, the pairwise interaction contains the high-order multipole interactions beyond the dipole moment interactions [4,6,7]. For the special quenched J moments with $J = 0$, the coupling with the excited J states could lead to an exciton Bose-Einstein condensation with magnetism [29,36]. In this paper, we show that, for the unquenched local moment J, the excitonic process to the excited J states appears *virtually* and renders an important correction of the superexchange interaction between the local moments, especially in the presence of external magnetic field.

Atomic eigenstates. – Because of the universality and the broad applicability of this virtual excitonic process, we deliver our theory via the simplest $J = 1/2$ local moment for the $4d^5$ or $5d^5$ electron configuration of the Ir^{4+} or Ru^{3+} ion in the octahedral crystal field environment. This occurs for example in many iridates such as Sr_2IrO_4. The five degenerate atomic d orbitals split into the t_{2g} and the e_g manifolds, with the former having lower energy. In the case of a large crystal field, the energy gap is large, leading to a low-spin d^5 configuration. There is one hole in the t_{2g} manifold which consists of orbitals d_{yz}, d_{zx}, and d_{xy}. The t_{2g} manifold has an effective orbital angular momentum $l_{\rm eff} = 1$ [37]. Because there is a single hole in the atomic ground state, we will use the hole representation in this paper. The atomic Hamiltonian in the t_{2g} subspace at site i is

$$H_{0i} = \frac{U}{2} {\sum_{mm'\sigma\sigma'}}' n^{(e)}_{im\sigma} n^{(e)}_{im'\sigma'} - \lambda \sum_{mm'\sigma\sigma'} \boldsymbol{l}_{mm'} \cdot \boldsymbol{s}_{\sigma\sigma'} c^\dagger_{im\sigma} c_{im'\sigma'}, \tag{1}$$

where $c^\dagger_{im\sigma}$ ($c_{im\sigma}$) is the hole creation (annihilation) operator with orbital $m = 1, 2, 3$ and spin $\sigma = \uparrow, \downarrow$ at site i. The first term is the Hubbard interaction with strength $U > 0$. The prime of the summation means that the term with $(m\sigma) = (m'\sigma')$ is excluded. Note that a hole creation (annihilation) operator is an electron annihilation (creation) operator. Thus, the electron occupation number $n^{(e)}_{im\sigma} = 1 - n_{im\sigma}$ in the hole representation. The Hund's interactions are relatively small and hence neglected. The last term is the spin-orbit interaction with strength $\lambda > 0$. In the hole representation, the sign before λ is negative. The orbital index $m = 1, 2, 3$ corresponds to the three t_{2g} orbitals d_{yz}, d_{zx}, and d_{xy}, respectively. In this index ordering, the orbital angular momentum matrix elements $(l_m)_{m'm''} = \mathrm{i}\epsilon_{mm'm''}$, in which $l_{1,2,3}$ refers to $l_{x,y,z}$, respectively. The sign is opposite to the matrix elements of the genuine $l = 1$ orbitals [37]. The spin angular momentum $\boldsymbol{s} = \boldsymbol{\sigma}/2$, where $\boldsymbol{\sigma} = (\sigma_x, \sigma_y, \sigma_z)$ is the vector of Pauli matrices.

The eigenstates of the SOC term are two $j_{\rm eff} = 1/2$ states with energy $-\lambda$, and four $j_{\rm eff} = 3/2$ states with energy $\lambda/2$. In the atomic limit, the hole lies on the two-fold degenerate $j_{\rm eff} = 1/2$ level, making the ion an effective spin-1/2 system. As long as the hoppings between different sites remain relatively weak as compared with the on-site Coulomb repulsion, the system remains a spin-orbit-coupled Mott insulator.

Exchange interaction. – The interactions between the effective spins have their origin in the virtual hopping processes. When the hopping terms between different sites are taken into account, there are virtual intermediate states that contain more than one hole on the same ion site, at the cost of Coulomb repulsion energy. The intermediate states are subject to the Pauli exclusion principle, which prevents two holes with the same spin from occupying the same state. Therefore, the resulting energy correction will be dependent on the spin configurations of the initial and finial states. The overall effect is the development of an effective interaction between neighboring spins, which is called exchange interaction.

In general, the hopping processes can be described by the Hamiltonian

$$T = \sum_{ij\sigma} C^\dagger_{i\sigma} h_{ij} C_{j\sigma}, \tag{2}$$

in which $h_{ij} = h^\dagger_{ji}$ is the matrix for the hopping from site j to site i, and $C^\dagger_{i\sigma} = [c^\dagger_{i,yz,\sigma}, c^\dagger_{i,zx,\sigma}, c^\dagger_{i,xy,\sigma}]$ is a row vector of the t_{2g} hole creation operators at site i with spin σ. The Hamiltonian of the entire system is $H = H_0 + T$, where $H_0 = \sum_i H_{0i}$ is the summation of the atomic Hamiltonian (1) on each site. For a Mott insulator, H_0 dominates T, so the latter can be treated by perturbation theory. The matrix element of the effective Hamiltonian up to third order is

$$(H_{\rm eff})_{mn} = (H_0)_{mn} + \sum_\alpha \frac{T_{m\alpha} T_{\alpha n}}{\omega_{0\alpha}} + \sum_{\alpha\beta} \frac{T_{m\alpha} T_{\alpha\beta} T_{\beta n}}{\omega_{0\alpha}\omega_{0\beta}}, \tag{3}$$

where the Latin indices m and n refer to the ground states of the unperturbed Hamiltonian H_0, and the Greek indices α and β refer to the excited states. $\omega_{0\alpha}$ is the difference between the unperturbed energies of the ground state 0 and the excited state α.

We begin by a simple model shown in fig. 1(a), in which the d^5 octahedrally coordinated transition metals arrange in a two-dimensional square lattice, the same as the CuO_2 plane in cuprates.

By symmetry considerations, the hopping matrices for $2 \to 1$ and $3 \to 1$ in fig. 1(a) have the form

$$h_{12} = \begin{bmatrix} t_\delta & 0 & 0 \\ 0 & t_\pi & 0 \\ 0 & 0 & t_\pi \end{bmatrix} \quad \text{and} \quad h_{13} = \begin{bmatrix} \frac{t'_\pi + t'_\delta}{2} & \frac{t'_\pi - t'_\delta}{2} & 0 \\ \frac{t'_\pi - t'_\delta}{2} & \frac{t'_\pi + t'_\delta}{2} & 0 \\ 0 & 0 & \frac{3t'_\sigma + t'_\delta}{4} \end{bmatrix}, \tag{4}$$

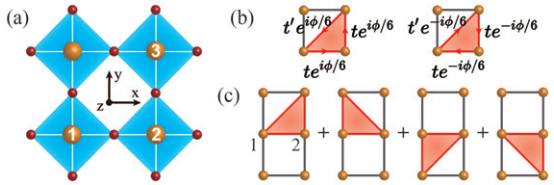

Fig. 1: (a) The square lattice of d^5 transition metals (orange balls) with corner sharing octahedra of oxygen ligands (red balls). Only the in-plane oxygen atoms are shown. (b) The Peierls phases attached to the hopping paths, where t (t') is some nearest-neighbor (next-nearest-neighbor) hopping parameter. (c) For the spin interaction between site 1 and site 2, there are four types of hopping path for the virtual excitonic process, represented by the red triangles.

respectively. Their subscripts hint that the hoppings are similar to the corresponding dd-type Slater-Koster parameters, although usually the ligand-mediated indirect hopping is the dominant mechanism. All the other hopping matrices up to second nearest neighbor can be derived by symmetry. The hopping terms for further neighbors are neglected.

Traditionally, the excited states are limited to the ones that have two holes lying on the same $j_{\rm eff} = 1/2$ manifold, similar to the one-band Hubbard model [38]. With this restriction, only the second-order perturbation term in eq. (3) contributes to the nearest-neighbor spin-spin interaction. By the definition of the spin operator at site i as $(\boldsymbol{S}_i)_{ss'} = c^\dagger_{is}\boldsymbol{\sigma}_{ss'}c_{is'}/2$ where s and s' refer to the two $j_{\rm eff} = 1/2$ states, the effective Hamiltonian for the spin interaction between site 1 and site 2 is derived as

$$H_{12} = \frac{4(2t_\pi + t_\delta)^2}{9U}\boldsymbol{S}_1 \cdot \boldsymbol{S}_2. \tag{5}$$

This is similar to the result for the one-band Hubbard model. If $t_\pi = t_\delta = t$, then the coefficient $4t^2/U$ is the expected antiferromagnetic Heisenberg exchange interaction parameter.

Virtual excitonic process. – In the spin-orbit-coupled Mott insulator the $j_{\rm eff} = 1/2$ level is not well separated from the $j_{\rm eff} = 3/2$ level, as can be seen in the typical spin-orbit-coupled Mott insulators Sr_2IrO_4 [39], Na_2IrO_3 [40], and α-$RuCl_3$ [12]. The existence of the nearby $j_{\rm eff} = 3/2$ level will have an impact on the spin exchange interaction.

After taking the $j_{\rm eff} = 3/2$ level into consideration, the intermediate excited states represented by the indices α and β in eq. (3) not only contain those in which two holes occupy the $j_{\rm eff} = 1/2$ level, but also those in which one hole occupies the $j_{\rm eff} = 1/2$ level and the other hole occupies the $j_{\rm eff} = 3/2$ level[1]. The process involving the latter type of excited states is called the virtual excitonic process, because it is as if one hole is excited from the $j_{\rm eff} = 1/2$ level to the $j_{\rm eff} = 3/2$ level, leaving an electron behind, and the virtual pair of the electron and the excited hole forms a virtual exciton.

[1]The intermediate states in which two holes occupy the $j_{\rm eff} = 3/2$ level appear only in higher order terms in the perturbative expansion.

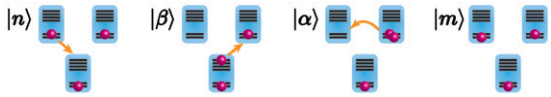

Fig. 2: An example of virtual excitonic process. Each blue rectangle represents a d^5 transition metal ion, which has a two-fold degenerate $j_{\rm eff} = 1/2$ level and a four-fold degenerate $j_{\rm eff} = 3/2$ level. $|n\rangle$ and $|m\rangle$ are the initial state and the final state, respectively. $|\beta\rangle$ and $|\alpha\rangle$ are two intermediate excited states.

Allowing the virtual excitonic process in the perturbation expansion (3), it is found that the correction to the two-spin exchange interaction comes from the third-order term, which involves the participation of a third ion, as schematically shown in fig. 2.

The involvement of a third ion has significant consequences when an out-of-plane magnetic field is applied. There will be additional Peierls phases in the hopping matrices. The accumulated Peierls phase for a closed loop should equal 2π times the magnetic flux through the loop area divided by the flux quantum hc/e. Assuming that the accumulated Peierls phase for a plaquette is ϕ, it is convenient to use the gauge indicated in fig. 1(b). Note that the second-order interaction (5) is independent of the magnetic field because the areas of the hopping paths $1 \to 2 \to 1$ and $2 \to 1 \to 2$ are zero.

For a square lattice up to second-nearest-neighbor hopping, fig. 1(c) shows the four hopping paths at the third perturbation order that contribute to the exchange interaction between site 1 and site 2. The resulting correction term is found to be

$$H'_{12} = \frac{16(\lambda + U)(2t_\pi + t_\delta)(t_\delta - t_\pi)(3t'_\sigma - 2t'_\pi - t'_\delta)}{9U(3\lambda + 2U)^2} \times \cos\frac{\phi}{2}\boldsymbol{S}_1 \cdot \boldsymbol{S}_2. \tag{6}$$

In sharp contrast to eq. (5), the correction term is dependent on the magnetic field. This is because the area of the third-order hopping processes like $1 \to 2 \to 3 \to 1$ is nonzero, leading to a nonvanishing magnetic flux. Such field dependence is fundamentally different from the Zeeman interaction, because it is essentially coupled to the magnetic flux, which is an orbital effect. The above analysis can be easily generalized to different lattice models, so the effect should be ubiquitous in various spin-orbit-coupled Mott insulators.

At the third-order perturbation, there are also the ring exchange interactions among each group of three neighboring spins. For the spins 1, 2, and 3 in fig. 1(a), the ring exchange interaction is

$$H_{123} = -\frac{-2\,(2t_\pi + t_\delta)^2\,(3t'_\sigma + 4t'_\pi + 5t'_\delta)}{9U^2}\sin\frac{\phi}{2}\,\boldsymbol{S}_1 \cdot (\boldsymbol{S}_2 \times \boldsymbol{S}_3)\,. \tag{7}$$

Because the mixed product of three spins breaks the time-reversal symmetry, the 3-spin ring exchange exists only when a magnetic field is applied. Hence, it must be field-dependent. The result (7) does not involve the virtual excitonic process. The hole only hops between the $j_{\rm eff} = 1/2$ states of the three ions. The corrections by the virtual excitonic process comes at the fourth perturbation order, which engages a fourth ion to provide the $j_{\rm eff} = 3/2$ states. We expect that the correction terms have a field dependence of $\sin\phi$, because the loop area is that of a plaquette, and the product $[\sin\phi\ \boldsymbol{S}_1 \cdot (\boldsymbol{S}_2 \times \boldsymbol{S}_3)]$ is time-reversal invariant.

Application to Sr_2IrO_4. – Having demonstrated the basic concept of the virtual excitonic process and the results on a simple model, we take a look at its effects in real material. To demonstrate it, we use Sr_2IrO_4 as an example. Sr_2IrO_4 is a well-known spin-orbit-coupled insulator [3,38,41]. The electron configuration of the Ir^{4+} ion is $5d^5$, the same as our assumption before. It consists of corner sharing IrO_6 octahedra layers with intervening Sr layers, see fig. 3(a). The crystal structure of Sr_2IrO_4 is the Ca_2MnO_4 type with space group $I4_1/acd$ [42]. Compared to the above simple model, the complication is that the IrO_6 octahedra rotate alternately from perfect alignment, as shown in fig. 3(b).

The TB model without SOC is still given by the form of eq. (2). But we note that here the d orbitals in the subscripts are defined with respect to the local coordinate system aligned with the IrO_6 octahedron at the corresponding site, as shown by the two sets of local coordinate systems $x'y'z'$ in fig. 3(b). On the contrary, the spin directions are defined with respect to the global xyz axes in fig. 3(b), because in the end we would like to have a spin interaction Hamiltonian expressed in the global coordinate system.

We perform the first-principles calculations to obtain the parameters in the Hubbard Hamiltonian. Wannier functions and the tight-binding model are constructed from the Kohn-Sham orbitals, and constrained random phase approximation is used to calculate the interaction parameter U. See details in the Supplementary Material `Supplementarymaterial.pdf` (SM), which includes refs. [42–54].

Considering the crystal symmetry, the hole hopping matrices between the nearest-neighbor pair 12 and the second-nearest-neighbor pair 13 in fig. 3(b) are

$$h_{12} = -\begin{bmatrix} -t_3 & t_4 & 0 \\ -t_4 & -t_1 & 0 \\ 0 & 0 & -t_2 \end{bmatrix} \text{ and } h_{13} = -\begin{bmatrix} t_3' & -t_4' & 0 \\ -t_4' & t_2' & 0 \\ 0 & 0 & -t_1' \end{bmatrix}, \tag{8}$$

respectively. The overall minus signs are to emphasize that the hopping matrices for holes differ from those for electrons by a sign, while the latter is the direct result of the first-principles calculations. We note that the zero matrix elements in h_{12} and h_{13} are not strict because of the interlayer interactions. However, their magnitudes are around 0.1 meV, much smaller than the other matrix elements. Thus, the smallness of these matrix elements reflects the weakness of the interlayer interactions. Other hopping matrices can be inferred by the crystal symmetry. The hopping parameters $t_{1,2,3,4}$ and $t'_{1,2,3,4}$, the SOC strength λ, and the Hubbard interaction parameter U are listed in table 1.

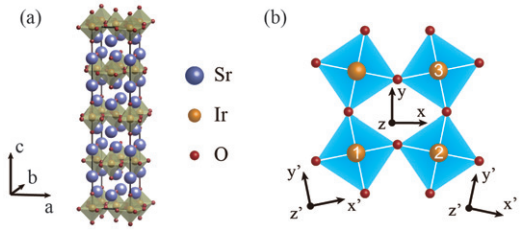

Fig. 3: (a) The conventional unit cell of Sr_2IrO_4. It is composed of four layers stacking along the c-direction. (b) A IrO_2 plane. The corner sharing IrO_6 octahedra rotate alternately, resulting in two sets of local coordinate systems $x'y'z'$.

Table 1: The parameters of the Hubbard model of Sr_2IrO_4 (top), and the parameters of the spin interaction between site 1 and site 2 in fig. 3(b) (bottom), in meV.

t_1	t_2	t_3	t_4	t_1'	t_2'	t_3'	t_4'	λ	U
285	243	46.8	27.8	125	30.1	5.92	11.1	365	2232
J	D	K	J'	D'	K'				
65.2	12.7	1.23	3.51	0.895	0.237				

By applying the perturbation theory, the spin interaction between the pair 12 in fig. 3(b) is found to be

$$\begin{aligned} H_{12} = {} & J\boldsymbol{S}_1 \cdot \boldsymbol{S}_2 - D(\boldsymbol{S}_1 \times \boldsymbol{S}_2)_z + KS_1^z S_2^z \\ & - [J'\boldsymbol{S}_1 \cdot \boldsymbol{S}_2 + D'(\boldsymbol{S}_1 \times \boldsymbol{S}_2)_z - K'S_1^z S_2^z] \Big\} \cos\frac{\phi}{2}. \end{aligned} \tag{9}$$

The analytical expressions for the coefficients are given in the SM, and their numerical values are listed in table 1. The terms involving J', D', and K' come from the virtual excitonic processes. The phase $\phi = eBl^2/\hbar$, where B is the out-of-plane magnetic field, and $l = 3.88$ Å is the distance between nearest-neighbor Ir atoms. The order of magnitude $\phi \sim 1$ corresponds to a magnetic field $B \sim 4.4 \times 10^3$ T.

Nonlinear susceptibility. – The positive coefficient before $S_1^z S_2^z$ leads to the easy-plane anisotropy. The in-plane magnetic structure is canted antiferromagnetic because of the competition between the Heisenberg and the Dzyaloshinskii-Moriya interaction (the first two terms of eq. (9)). With the application of a magnetic field $\boldsymbol{B}$ perpendicular to the IrO_2 layers, the canted antiferromagnetic structure develops an out-of-plane component. We first neglect the virtual excitonic process corrections, then

the classical energy per site is

$$E = 2\left[J\boldsymbol{S}_{\rm A}\cdot\boldsymbol{S}_{\rm B} - D\left(\boldsymbol{S}_{\rm A}\times\boldsymbol{S}_{\rm B}\right)_z + KS^z_{\rm A}S^z_{\rm B}\right] - 2\mu_{\rm B}BS^z_{\rm A}, \tag{10}$$

where $\boldsymbol{S}_{\rm B}$ and $\boldsymbol{S}_{\rm B}$ are the spins on the two sublattices, with the same z component, and $\mu_{\rm B}$ is the Bohr magneton. We have used the fact that the Landé g-factor of the $j_{\rm eff}=1/2$ hole state is -2. By minimizing the energy, the tilting angle of the spins away from the xy plane can be obtained, and the perpendicular magnetic susceptibility is found to be

$$\chi_\perp = \frac{N\mu_{\rm B}^2}{\sqrt{J^2+D^2}+J+K}, \tag{11}$$

in which N is the site density. This result (11) has the same property as the mean-field result for the Néel antiferromagnetism that below the Néel temperature it depends neither on the temperature nor on the magnetic field.

Now we take into account the correction term from the virtual excitonic process. It amounts to the replacements $J\to J-J'\cos(\phi/2)$, $D\to D+D'\cos(\phi/2)$, and $K\to K+K'\cos(\phi/2)$. With Taylor expansion up to $O(\phi^2)$, we find the magnetization

$$M = \chi_\perp^{(1)}B + \chi_\perp^{(3)}B^3 + \cdots, \tag{12}$$

where

$$\chi_\perp^{(1)} = \frac{N\mu_{\rm B}^2}{\sqrt{(J-J')^2+(D+D')^2}+J-J'+K+K'} \tag{13}$$

is linear susceptibility, and

$$\chi_\perp^{(3)} = -\frac{N\mu_{\rm B}^2\left[\frac{(J-J')J'-(D+D')D'}{\sqrt{(J+J')^2+(D-D')^2}}+J'-K'\right]\left(\frac{el^2}{\hbar}\right)^2}{8\left[\sqrt{(J-J')^2+(D+D')^2}+J-J'+K+K'\right]^2} \tag{14}$$

is the nonlinear susceptibility [55,56]. Its existence is the consequence of the virtual excitonic process. This clarifies one important source of the nonlinear susceptibility in these systems.

Discussion. – Here we discuss the applicability of the excitonic superexchange. We have shown that the virtual excitonic process appears in the high-order perturbation theory of the multiple-band Hubbard model. A smaller spin-orbit-coupling and/or a weak Hubbard interaction could enhance its contribution. Apparently, in many of these $4d/5d$ magnets, the spin-orbit coupling is not really the dominant energy scale, and the systems also behave like weak Mott insulators. The $4d$ magnet α-$RuCl_3$ is a good example of this kind. This material shows a remarkable thermal Hall transport result in external magnetic fields, which is likely to be related to the gapped Kitaev spin liquid [57–59]. More recently, it has been found that its thermal conductivity oscillates when an external magnetic field is applied [60]. It is believed that the oscillation originates from the existence of the spinon Fermi surface of some kind. The orbital quantization of the spinons requires the coupling of the spinons with an internal $U(1)$ gauge field [61]. Such orbital effect is obviously not controlled via the Zeeman term. The virtual excitonic process and/or the strong charge fluctuation could provide the microscopic means to lock the internal $U(1)$ gauge field with the external magnetic flux, and thereby generating the oscillatory behaviors.

For the Co-based Kitaev materials [22–26], the Hubbard interaction is large, but the spin-orbit coupling is weak. Thus, the excitonic superexchange may still be important. For the rare-earth magnets, the crystal field enters as an important energy scale. If the crystal field energy separation between the ground states and the excited states is not large enough compared to the exchange energy scale, the excited states would be involved into the low-temperature magnetic physics. This upper-branch magnetism has been invoked for the pyrochlore magnet $Tb_2Ti_2O_7$ [62–65].

The concept could also be applied to systems such as metal organic frameworks, molecular magnets, and Moiré systems, which have large lattice constants. Another example is the spin-liquid candidate material 1T-TaS_2 [66–70], which enters into a charge-density-wave (CDW) phase at low temperature. In the CDW phase, each supercell has a localized unpaired electron which provides the spin. The neighboring spins are separated at a distance l larger than ten angstroms. Moreover, the orbitals d_{xy}, $d_{x^2-y^2}$, and d_{z^2} have similar energies [71], which facilitates the excitonic process. The required magnetic field B for the phase $\phi\sim eBl^2/\hbar$ to be at the order of $O(1)$ drops to hundreds of tesla, making the effect of excitonic process more prominent.

* * *

The first-principles calculations for this work were performed on TianHe-2. We are thankful for the support from the National Supercomputing Center in Guangzhou (NSCC-GZ). This work is supported by the National Science Foundation of China with Grant No. 92065203, the Ministry of Science and Technology of China with Grants No. 2018YFE0103200, by the Shanghai Municipal Science and Technology Major Project with Grant No. 2019SHZDZX01, and by the Research Grants Council of Hong Kong with General Research Fund Grant No. 17306520.

REFERENCES

[1] Witczak-Krempa W., Chen G., Kim Y. B. and Balents L., *Annu. Rev. Condens. Matter Phys.*, **5** (2014) 57.

[2] Chen G. and Balents L., *Phys. Rev. B*, **78** (2008) 094403.

[3] Jackeli G. and Khaliullin G., *Phys. Rev. Lett.*, **102** (2009) 017205.
[4] Chen G., Pereira R. and Balents L., *Phys. Rev. B*, **82** (2010) 174440.
[5] Chaloupka J. c. v., Jackeli G. and Khaliullin G., *Phys. Rev. Lett.*, **105** (2010) 027204.
[6] Chen G. and Balents L., *Phys. Rev. B*, **84** (2011) 094420.
[7] Chen G. and Balents L., *Phys. Rev. B*, **91** (2015) 219903.
[8] Chaloupka J. c. v., Jackeli G. and Khaliullin G., *Phys. Rev. Lett.*, **110** (2013) 097204.
[9] Rau J. G., Lee E. K.-H. and Kee H.-Y., *Phys. Rev. Lett.*, **112** (2014) 077204.
[10] Kim H.-S., Shankar V. Vijay, Catuneanu A. and Kee H.-Y., *Phys. Rev. B*, **91** (2015) 241110.
[11] Rau J. G., Lee E. K.-H. and Kee H.-Y., *Annu. Rev. Condens. Matter Phys.*, **7** (2016) 195.
[12] Plumb K. W., Clancy J. P., Sandilands L. J., Shankar V. V., Hu Y. F., Burch K. S., Kee H.-Y. and Kim Y.-J., *Phys. Rev. B*, **90** (2014) 041112.
[13] Trebst S., *Kitaev materials*, arXiv:1701.07056 [cond-mat.str-el] (2017).
[14] Hermanns M., Kimchi I. and Knolle J., *Annu. Rev. Condens. Matter Phys.*, **9** (2018) 17.
[15] Rau J. G. and Gingras M. J., *Annu. Rev. Condens. Matter Phys.*, **10** (2019) 357.
[16] Li Y.-D., Wang X. and Chen G., *Phys. Rev. B*, **94** (2016) 035107.
[17] Liu C., Huang C.-J. and Chen G., *Phys. Rev. Res.*, **2** (2020) 043013.
[18] Li Y.-D. and Chen G., *Phys. Rev. B*, **95** (2017) 041106.
[19] Li Y.-D., Wang X. and Chen G., *Phys. Rev. B*, **94** (2016) 201114.
[20] Savary L., Wang X., Kee H.-Y., Kim Y. B., Yu Y. and Chen G., *Phys. Rev. B*, **94** (2016) 075146.
[21] Rau J. G., Wu L. S., May A. F., Poudel L., Winn B., Garlea V. O., Huq A., Whitfield P., Taylor A. E., Lumsden M. D., Gingras M. J. P. and Christianson A. D., *Phys. Rev. Lett.*, **116** (2016) 257204.
[22] Liu H., Chaloupka J. and Khaliullin G., *Phys. Rev. Lett.*, **125** (2020) 047201.
[23] Das S., Voleti S., Saha-Dasgupta T. and Paramekanti A., *Phys. Rev. B*, **104** (2021) 134425.
[24] Liu H., *Int. J. Mod. Phys. B*, **35** (2021) 2130006.
[25] Liu H. and Khaliullin G., *Phys. Rev. B*, **97** (2018) 014407.
[26] Sano R., Kato Y. and Motome Y., *Phys. Rev. B*, **97** (2018) 014408.
[27] Chamorro J. R., Ge L., Flynn J., Subramanian M. A., Mourigal M. and McQueen T. M., *Phys. Rev. Mater.*, **2** (2018) 034404.
[28] Chen G., *Phys. Rev. B*, **96** (2017) 020412.
[29] Li F.-Y. and Chen G., *Phys. Rev. B*, **100** (2019) 045103.
[30] Buessen F. L., Hering M., Reuther J. and Trebst S., *Phys. Rev. Lett.*, **120** (2018) 057201.
[31] Das S., Nafday D., Saha-Dasgupta T. and Paramekanti A., *Phys. Rev. B*, **100** (2019) 140408.
[32] Gao Y. H., Hickey C., Xiang T., Trebst S. and Chen G., *Phys. Rev. Res.*, **1** (2019) 013014.
[33] Zhou X., Li H., Waugh J. A., Parham S., Kim H.-S., Sears J. A., Gomes A., Kee H.-Y., Kim Y.-J. and Dessau D. S., *Phys. Rev. B*, **94** (2016) 161106.
[34] Sandilands L. J., Tian Y., Reijnders A. A., Kim H.-S., Plumb K. W., Kim Y.-J., Kee H.-Y. and Burch K. S., *Phys. Rev. B*, **93** (2016) 075144.
[35] Maekawa S., Tohyama T., Barnes S., Ishihara S., Koshibae W. and Khaliullin G., *Physics of Transition Metal Oxides* (Springer-Verlag, Berlin, Heidelberg) 2003.
[36] Khaliullin G., *Phys. Rev. Lett.*, **111** (2013) 197201.
[37] Abragam A. and Bleaney B., *Electron Paramagnetic Resonance of Transition Ions* (Oxford University Press) 1970.
[38] Wang F. and Senthil T., *Phys. Rev. Lett.*, **106** (2011) 136402.
[39] Kim B. J., Jin H., Moon S. J., Kim J.-Y., Park B.-G., Leem C. S., Yu J., Noh T. W., Kim C., Oh S.-J., Park J.-H., Durairaj V., Cao G. and Rotenberg E., *Phys. Rev. Lett.*, **101** (2008) 076402.
[40] Comin R., Levy G., Ludbrook B., Zhu Z.-H., Veenstra C. N., Rosen J. A., Singh Y., Gegenwart P., Stricker D., Hancock J. N., van der Marel D., Elfimov I. S. and Damascelli A., *Phys. Rev. Lett.*, **109** (2012) 266406.
[41] Engström L., Pereg-Barnea T. and Witezak-Krempa W., *Phys. Rev. B*, **103** (2021) 155147.
[42] Huang Q., Soubeyroux J., Chmaissem O., Sora I., Santoro A., Cava R., Krajewski J. and Peck W., *J. Solid State Chem.*, **112** (1994) 355.
[43] Marzari N. and Vanderbilt D., *Phys. Rev. B*, **56** (1997) 12847.
[44] Souza I., Marzari N. and Vanderbilt D., *Phys. Rev. B*, **65** (2001) 035109.
[45] Hohenberg P. and Kohn W., *Phys. Rev.*, **136** (1964) B864.
[46] Kohn W. and Sham L. J., *Phys. Rev.*, **140** (1965) A1133.
[47] Giannozzi P., Baroni S., Bonini N., Calandra M., Car R., Cavazzoni C., Ceresoli D., Chiarotti G. L., Cococcioni M., Dabo I., Dal Corso A., de Gironcoli S., Fabris S., Fratesi G., Gebauer R., Gerstmann U., Gougoussis C., Kokalj A., Lazzeri M., Martin-Samos L., Marzari N., Mauri F., Mazzarello R., Paolini S., Pasquarello A., Paulatto L., Sbraccia C., Scandolo S., Sclauzero G., Seitsonen A. P., Smogunov A., Umari P. and Wentzcovitch R. M., *J. Phys.: Condens. Matter*, **21** (2009) 395502.
[48] Giannozzi P., Andreussi O., Brumme T., Bunau O., Buongiorno Nardelli M., Calandra M., Car R., Cavazzoni C., Ceresoli D., Cococcioni M., Colonna N., Carnimeo I., Dal Corso A., de Gironcoli S., Delugas P., DiStasio R. A. jr., Ferretti A., Floris A., Fratesi G., Fugallo G., Gebauer R., Gerstmann U., Giustino F., Gorni T., Jia J., Kawamura M., Ko H.-Y., Kokalj A., Küçükbenli E., Lazzeri M., Marsili M., Marzari N., Mauri F., Nguyen N. L., Nguyen H.-V., Otero-de-la-Roza A., Paulatto L., Poncé S., Rocca D., Sabatini R., Santra B., Schlipf M., Seitsonen A. P., Smogunov A., Timrov I., Thonhauser T., Umari P., Vast N., Wu X. and Baroni S., *J. Phys.: Condens. Matter*, **29** (2017) 465901.

[49] Schlipf M. and Gygi F., *Comput. Phys. Commun.*, **196** (2015) 36.
[50] Hamann D. R., *Phys. Rev. B*, **88** (2013) 085117.
[51] Aryasetiawan F., Miyake T. and Sakuma R., *The constrained RPA method for calculating the Hubbard U from first-principles*, in *The LDA+DMFT Approach to Strongly Correlated Materials*, edited by Pavarini E., Koch E., Vollhardt D. and Lichtenstein A. (Forschungszentrum Jülich GmbH, Institute for Advanced Simulations, Jülich) 2011.
[52] Nakamura K., Yoshimoto Y., Nomura Y., Tadano T., Kawamura M., Kosugi T., Yoshimi K., Misawa T. and Motoyama Y., *Comput. Phys. Commun.*, **261** (2021) 107781.
[53] Hinuma Y., Pizzi G., Kumagai Y., Oba F. and Tanaka I., *Comput. Mater. Sci.*, **128** (2017) 140.
[54] Togo A. and Tanaka I., Spglib: *a software library for crystal symmetry search*, arXiv:1808.01590 [cond-mat.mtrl-sci] (2018).
[55] Fujiki S. and Katsura S., *Prog. Theor. Phys.*, **65** (1981) 1130.
[56] Machida Y., Nakatsuji S., Onoda S., Tayama T. and Sakakibara T., *Nature*, **463** (2010) 210.
[57] Yokoi T., Ma S., Kasahara Y., Kasahara S., Shibauchi T., Kurita N., Tanaka H., Nasu J., Motome Y., Hickey C. *et al.*, *Science*, **373** (2021) 568.
[58] Kasahara Y., Sugii K., Ohnishi T., Shimozawa M., Yamashita M., Kurita N., Tanaka H., Nasu J., Motome Y., Shibauchi T. *et al.*, *Phys. Rev. Lett.*, **120** (2018) 217205.
[59] Kasahara Y., Ohnishi T., Mizukami Y., Tanaka O., Ma S., Sugii K., Kurita N., Tanaka H., Nasu J., Motome Y. *et al.*, *Nature*, **559** (2018) 227.
[60] Czajka P., Gao T., Hirschberger M., Lampen-Kelley P., Banerjee A., Yan J., Mandrus D. G., Nagler S. E. and Ong N. P., *Nat. Phys.*, **17** (2021) 915.
[61] Motrunich O. I., *Phys. Rev. B*, **73** (2006) 155115.
[62] Gaulin B. D., Gardner J. S., McClarty P. A. and Gingras M. J. P., *Phys. Rev. B*, **84** (2011) 140402.
[63] Molavian H. R., Gingras M. J. P. and Canals B., *Phys. Rev. Lett.*, **98** (2007) 157204.
[64] Liu C., Li F.-Y. and Chen G., *Phys. Rev. B*, **99** (2019) 224407.
[65] Kadowaki H., Wakita M., Fåk B., Ollivier J. and Ohira-Kawamura S., *Phys. Rev. B*, **105** (2022) 014439.
[66] Law K. T. and Lee P. A., *Proc. Natl. Acad. Sci. U.S.A.*, **114** (2017) 6996.
[67] He W.-Y., Xu X. Y., Chen G., Law K. T. and Lee P. A., *Phys. Rev. Lett.*, **121** (2018) 046401.
[68] Butler C. J., Yoshida M., Hanaguri T. and Iwasa Y., *Nat. Commun.*, **11** (2020) 2477.
[69] Wang Y. D., Yao W. L., Xin Z. M., Han T. T., Wang Z. G., Chen L., Cai C., Li Y. and Zhang Y., *Nat. Commun.*, **11** (2020) 4215.
[70] Li C.-K., Yao X.-P., Liu J. and Chen G., *Phys. Rev. Lett.*, **129** (2022) 017202.
[71] Rossnagel K. and Smith N. V., *Phys. Rev. B*, **73** (2006) 073106.